Finite element modelling of innovative interspinous process spacers for the lumbar spine

Valentina da Silva Carvalho
valentina.carvalho@tecnico.ulisboa.pt

Instituto Superior Técnico, Lisboa, Portugal

October 2019

Abstract

Low back pain is an emerging problem in society. This occurs as lumbar spine is a leaning site for spinal diseases to occur. Their diagnostic and treatment have a large impact in countries' economics.
The number of spinal fusion surgeries for treatment of spinal diseases as herniation, stenosis and spondylolisthesis has increased. Interspinous posterior fixation has been proposed as a less invasive alternative to older systems for these spinal procedures. The motivation for this thesis comes directly from that fact, the surgical procedure can be not efficient, thus new design proposals can be achieved with this type of studies, to facilitate whole process.
This study had two main objectives that were achieved with the development of a new Finite Element model of L3-L5 spinal segment: i) study spinal degeneration process; ii) evaluation of a new design of innovative interspinous spacer to be inserted with lower risk for the patient, while having the same biomechanical performance as the existing device, Axle®.
The FE analysis have shown that new devices designs can be considered without resulting in a lower biomechanical performance, confirming that the study and development of a new interspinous devices can be extremely important, as spinal surgery can become less invasive and facilitated procedure. This thesis has also achieved to add more knowledge to the spinal degeneration process studies. All these results can be an important basis for the future research on new models of degenerative spinal process, as in the study of new designs and/or improvements of Axle device.

Keywords: Low Back Pain; Spinal Fusion; Interverbal Disc; Interspinous Posterior Fixation; Spinal Degeneration; Finite Elements

1. Introduction

Low back pain affects a large portion of the population, resulting in high care costs for therapy and treatment, especially in western societies. Currently, this problem is one of the major reasons for work absenteeism and productivity decrease, denoting itself to be an alert for society [1]. The big portion of clinical low back pain is explained by the aging of the population and how age is associated with degenerative spinal diseases that can cause spinal stenosis.
Today's, treatments of degenerative spinal diseases are mainly physical and medical, although these traditional methods may fail to cure the diseases and acts only to symptoms relieve. Therefore, surgical approaches should be applied to recover healthy functionality of the spine [2]. The causes for the degeneration of the spine are still unclear. Many of correlations with the intervertebral disc degeneration, facet joints and ligaments hypertrophy has been documented. The lack of an accepted explanatory models limits the understanding of this disease and retards the development of effective therapies [3].
Surgery for spinal stenosis generally consists of decompression of the nerves that are being compressed. This method can cause spine instability and consequently it is often followed by the introduction of some type of biomechanical device, in order to stabilize the spine, as well as to replace any kind of structure that have demonstrated to be very degenerated [4].
During the surgery intervention, specific attention should be paid to nerve root. Therefore, there is a high need to develop a less invasive spinal surgery technique. Thus, instrumentation is one of the main factors for design constraints and approaches of biomechanical devices, as fixation and fusion devices for stabilization of human spine [4].
A variety of interspinous fusion systems have been designed as minimally invasive devices after specific decompression surgeries. Different materials and models are available in the medical market, for

example the Axle® device. However, the main goal of todays is to create the ideal device that can provide robust posterior fixation with adjustable length. This type of mechanism could enable device-expansion and compression, allowing not only an easier device implementation, but also providing immobilization and stabilization of the spine, preserving the natural anatomy [5,6,7].

There are a lot of devices in the market that can guarantee spinal fusion. However, in the past years, there has been some progression in order to simplify the device implementation, minimize natural anatomy damages, and guarantee high efficiency of the spinal fusion procedure. Accordingly, the three main objectives (the first to reach the remaining two) of this study focus on:

1. Development and validation of a new FE model of a L3-L5 segment. It was intended that the developed model would be the most similar with the real geometry, simulating the intended results more accurately.
2. Simulate different spinal degenerations stages and analyze its effects for the spinal column.
3. Study of a new spinal fusion device, Device 2, that could be more easily implemented without compromising its biomechanical performance, and mechanical comparison with an existing one, Axle, an interspinous fusion system of X-Spine Systems, Inc, that will be mentioned as Device 1.

2. Background

The spinal fusion was initially introduced by Hibbs Albee in 1911 [1]. After that, this technique has been one of the most frequent mechanisms for treating spine diseases as deformity, trauma, degenerative disc disease and spondylolisthesis.

These devices must provide enough stiffness for spinal fusion and also must have an uncomplicated and safe process of insertion.

In order to minimize these possibilities and guarantee the efficiency of spinal fusion devices, there have been some progressions in the past years regarding their design and material composition.

Pedicle screw systems are one of the first and current techniques used in this particular type of spinal fusion. These pedicle screws are placed above and below the vertebrae, the screws are inserted through the pedicles and into the vertebral body, one on each side.

Several types of pedicle screw systems have been used in lumbar spine fusion. The first systems were made of stainless steel, but titanium-alloy devices have recently been developed and available on the market [2,3]. More recently, some authors have associated the pedicle screw systems to several drawbacks, such as imposing high mechanical stress on the adjacent segment due to the high restriction of the natural mobility which often leads to long-term degenerative changes, resulting in a need for additional fusion surgery [2,3]. Loosening and failure of some pedicle screws has also been reported.

The need for less invasive techniques and instrumentation has great importance in the fusion implants design constraints and approaches. Therefore, more recently, a variety of interspinous spacers have been proposed as minimally invasive devices that are promoted either as stabilization or fusion devices after specific decompression surgeries [4]. The Axle Interspinous Fusion System of X-spine Systems, Inc©. represented in Figure 1, is one of the devices commonly used for internal fixation of the lumbar spine. Axle is used for plate fixation and attachment to spinous processes. Several sizes of this implant are available becoming possible a good adaptation to consider the pathology and anatomy of the patients.

Figure 1: Illustration of the Axle device implemented into spinal segment. Retrieved from [14].

3. Implementation

3.1 Intact Model

The model was constructed from CT images through image segmentation, using the software ITK-SNAP® (University of Pennsylvania and University of Utah, USA). CT images from a healthy 40-year woman were obtained from the xVertSeg Database from Laboratory of Imaging Technologies (University of Ljubljana, Faculty of Electrical Engineering, Slovenia) [5]. ITK-SNAP® software permitted the image processing and segmentation. The images were segmented based on X-ray attenuation to separate soft tissue from the hard tissue by thresholding. The segmented, digitalized images provided a 3D volume.

A 3D model, in STL format, was obtained and imported to SolidWorks® (Dassault Systèmes SolidWorks, SolidWorks Corp., USA), as a solid model. Here, the two IVD were constructed through the interpolation of the vertebrae L3-L4 and L4-L5, since they were not obtained in the segmentation as the IVD density is lower when compared to bone. The two IVDs were also divided into nucleus pulposus and annulus fibrous, representing 70% and 30% of the disc, respectively [6].

Using SolidWorks software, it was also possible to design the facet joint, since the 3D volume of the vertebrae provided from the segmentation was considered as one single piece, which it is not

anatomically correct. Thus, a gap with 2 mm was created mimicking the joint between the inferior articular process and the superior articular process of the subsequent vertebrae [7].
The final model was then imported as Parasolid into FE solver ABAQUS® (Dassault Systèmes Simulia Corp., USA), in order to perform the FE analysis.
The properties parameters chosen for the FE analysis are showed in Table 1.
The vertebrae were not separated into cortical and trabecular bone, and the endplates were not considered as well, since this division would not add more relevant information to the wanted results. Furthermore, it would only add more complexity to the analysis.

Table 1: Material properties for the FE analysis.

Material	Formulation	Parameters	Ref.
Cortical Bone	Linear Elastic	E=1200 Mpa	[8]
		ν=0.3	
Nucleus Pulposus	Hyperelastic Isotropic (Mooney-Rivlin)	$C10$=0.12	[8]
		$C01$=0.03	
		$D1$=0.6667	
Annulus Fibrosus	Hyperelastic Anisotropic (Holzapfel)	$C10$=0.315	[9]
		$D1$=0.2540	
		$K1$=12 MPa	[10]
		$K2$= 300	
		$Kappa$= 0.1	[9]

The interactions between all parts of the model (three vertebrae and respective IVDs) were considered rigidly bonded using the tool merge geometry (selecting the option retain intersecting bound). The contacts between the facet joints were defined as surface-to-surface, soft contact with exponential-pressure-overclosure option available in Abaqus ®. This option was based on the literature, the contact parameters were adopted until reach the optimal values. Pressure of 50 N/mm^2 and clearance of 1 mm were the parameters that better fit the model under study [7].
In the top surface of the L3, it was defined a reference point which was coupled to all surface. This allowed that the loads were uniformly distributed on the surface.
After the mesh generation, the complete model consisted of 311 128 nodes and 210 235 elements that represented the L3-L5 segment of the lumbar spine. The number of elements was stipulated according to a convergence analysis. The element type chosen was quadratic tetrahedral with ten nodes (C3D10) mesh
All ligaments were modelled in ABAQUS as lines between two nodes (ligaments origin and insertion points were not personalized, their selection was selected based on anatomical and histological findings) with linear elastic behaviors and only tension response. Although ligaments represent nonlinear elastic behavior, in this model, they were considered as linear elastic to guarantee the simplicity of the simulation. Material properties and cross-sectional areas were adopted from literature as described in Table 2. [11,12,13]. Its achievement was accomplished through a material verification. Since all ligaments are attached along the spine, it was crucial necessary to define the local areas where the ligaments were attached to the vertebrae and IVD. The delimitation of these areas was made so that there was a strict agreement between the computational model and the anatomical reference. Thus, the nodes used to create the ligaments were coupled to the insertion area using the coupling constrain given by ABAQUS. This interaction guaranteed that all ligaments were attached to the insertion area and that the forces were uniformly distributed on the surface, simulating what occurs in a real human spine. The FE model with ligaments representations is shown in Figure 2.

Table 2: Materials properties for the spinal ligaments.

Liga-mments	E (MPa)	Ref.	Cross-sectional area (mm^2)	Ref.
ALL	20.0	[11]	75.9	[12]
PLL	10.0		1.6	[13]
CL	7.5		19.0	
FL	13.0		39.0	
ITL	12.0		1.8	
ISL	9.8		12.0	
SSL	8.8		6.0	

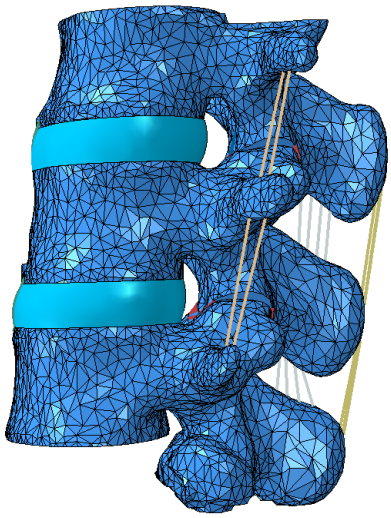

Figure 2: FE model with some of the ligaments represented.

3.2 Degenerative Models

In order to simulate the degeneration of the intervertebral discs, which mimic an unhealthy spine column, that can originate spinal stenosis, the healthy model was modified to simulate three different types of degeneration. The three unhealthy cases were created by assigning and combining two different degeneration stages (mild and moderate) for each of the discs with the healthy state. This combination was done considering that instrumentation will be performed at L3-L4 level.
The disc height was not reduced in order to simulate the condition after decompression at surgery time. Also, no changes were made to ligaments or other structures that could also cause spinal diseases.
The level of degeneration was simulated by modifying the material properties of the annulus ground substance and nucleus, mimicking the increased stiffness due to disc dehydration, and the loss of the annular fibers strength, simulating the laxity in the embedded annular fibers. The material parameters are described in Table 3.

Table 3: Material properties of the AF and NP for the considered degeneration stages.

	Annulus Fibrosus	**Fibers Properties**	**Nucleus Pulposus**
Healthy	C10= 0.315 D1=0.254	K1=12Mpa K2=300	C10=0.120 C01=0.030 D1=0.667
Mild	C10= 0.500 D1=0.320	K1=1.74Mpa K2=43.5	C10=0.168 C01=0.042 D1=0.476
Moderate	C10= 1.130 D1=0.140	K1=0.435Mpa K2=8.7	C10=0.221 C01=0.055 D1=0.723
Fibers I	C10= 0.315 D1=0.254	K1=1.74Mpa K2=43.5	C10=0.120 C01=0.030 D1=0.667
Fibers II	C10= 0.315 D1=0.254	K1=0.435Mpa K2=8.7	C10=0.120 C01=0.030 D1=0.667

3.3 Devices Model

According to ASTM F2077, a test method for intervertebral body fusion devices was done for the mechanical verifications of these implants.
For all analysis, the test loads are applied following the oblique direction in the posterior-anterior direction to simulate a real load situation provided for the normal curvature of the column [48,49].
Since, some of the work goes through a comparison of a concept, not a device, with an already existing device that has proven safety and clinical results, the tests to first validate the concept were static compression test and static shear test.
The 3D model of the Axle was created with SolidWorks according with information available in literature [14]. This file was imported to ABAQUS® solver in order to proceed with the FE analysis. The innovative design was kindly provided by the Clinlinc company, and also imported to ABAQUS.
For both devices, the contact between each device constituents were defined as surface-to-surface, normal behavior with hard contact option available in ABAQUS®. The material was assigned, with the propertied described in the Table 4. In addition, reference points were added at strategic locations in order to apply the desired loads later, considering the two type of mechanical tests. These reference points were coupled to the entire surface where the load application was intended. The location of the load application and boundary conditions was different according to the type of mechanical tests.

Table 4: Material properties of the Axle FE model.

Material	**Formulation**	**Parameters**	**Reference**
Titanium Alloy	Linear Elastic	E=105 000 MPa	[15]
		v=0.34	

3.4 Instrumented Models

First, the devices were placed in the L3-L4 interspinous segment as described in the X-Spine℠ Surgical Technique, using SolidWorks. The vertebrae were cut by the models to open space for the insertion's peaks. However, all peaks were simplified becoming curvilinear and not sharpened for better computational efficiency. Then, the models were imported to ABAQUS solver to perform the FE analysis. The material assigned to each part of the assembly were the same as in the healthy model, adding only the device, which was already mentioned in the previous section consists of a titanium alloy.
Although some authors argue that posterior tensioning by preservation or reconstruction of the posterior axial ligaments is advantageous, many surgeons do not do it, so 3 of the 7 ligaments placed in the intact model were removed to simulate the postoperative state. The removed ligaments were SSL, ISL and FL [1,16].
A reference point was created in the upper surface of L3, to apply the load. This point was coupled to the entire upper surface of the vertebra so that the load could be evenly distributed through the entire surface. The constraints used for the bone-insertion peaks interface were a tie constraint, ensuring that the two surfaces did not have any motion relatively to each other. The loads used in this work were chosen regarding the evaluation of physiological motions, so it was considered the lateral bending, flexion, extension and axial rotation [17]. All the moments

Table 4: Resume of all models that were constructed to guarantee the goal achievements for the study.

Case	L3-L4 Segment	L4-L5 Segment
1	Healthy IVD	Healthy IVD
2	Mild IVD	Healthy IVD
3	Mild IVD	Mild IVD
4	Moderate IVD	Mild IVD
5	Fibers I IVD	Healthy IVD
6	Fibers II IVD	Healthy IVD
2 with Device 1 Implemented	Mild IVD with Device 1 Implemented	Healthy IVD
2 with Device 2 Implemented	Mild IVD with Device 2 Implemented	Healthy IVD
3 with Device 1 Implemented	Mild IVD with Device 1 Implemented	Mild IVD
3 with Device 2 Implemented	Mild IVD with Device 2 Implemented	Mild IVD
4 with Device 1 Implemented	Moderate IVD with Device 1 Implemented	Mild IVD
4 with Device 2 Implemented	Moderate IVD with Device 2 Implemented	Mild IVD

applied were combined with a pre-load of 500N. This compressive pre-load was added to mimic the action of the muscles that were not included in the FE model. The option "follow nodal rotation" was used to simulate the compressive pre-load as a followed load [7,18]. After the preload application, the FE model was exposed to the physiological moments (flexion/extension, lateral bending, axial rotation) with 7.5Nm[18,17,19].

To summarize all models that were created and simulated in this work, Table 5 presents all information.

4. Results and Discussion

This chapter has three sets of results achieved from the three problems described in the section 1. The first is the analysis of the mechanical tests' results (compression and shear) done to guarantee the new device's robustness when compared to the Axle device already available for medical use. The second is the biomechanics analysis and understanding how different levels of IVD degeneration can influence and impact the spinal column. The last is the comparison of the two implemented devices into the L3-L4 spinal segment and conclusion relative to their biomechanical performance.

4.1 Devices

In order to evaluate the possible safety of Device 2, by comparing it to Device 1 (already with adequate biomechanical performance proven), FE analysis were performed according to ASTM F2077.

Studying Figure 3, it is possible to verify with the warmer coloration observed in the compression test, that this load case has more representative effects on both devices.

It is also possible to point out the critical points of each device. For both mechanical tests, it is concluded that the stress concentration occurs in the same locations for both devices: load application and constrained nodes for both cases, surrounding the fixation system for the Device 1, and rack teeth for the Device 2.

These stress concentrations should be avoided and require further attention from the devices' manufacturer.

In the device interface area where loads are applied and where its fixation is defined, there is a noticeable stress concentration. This is because, given the design of these structures, the stress value on these nodes will increase with the mesh refinement to infinite. This is unavoidable, and should be examined with special attention, since the points of load application and attachment are not the same in vivo applications and in this in silico analysis. However, the fact that it is not possible to better mimic boundary conditions leads to this option, disregard these values as maximum stress values of the device and evaluate other critical zones of interest. This being said, the study of maximum stress values was performed for both mechanical tests.

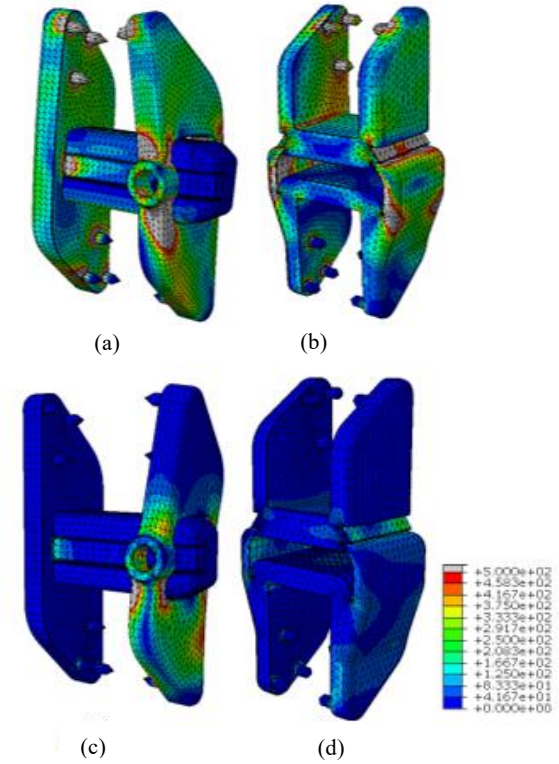

Figure 3: Mechanical tests results (S Von Mises); (a) Compression test result for Device 1; (b) Compression test result for Device 2; (c) Shear test result for Device 1; (d) Shear test result for Device 2.

For the compression test, the stress values were higher for the new device. In addition, it was found that these high values have been observed in the rack area where there is contact between the upper and lower gear rack teeth. Thus, the device 2 proves to be less stable, with large areas of stress concentration. However, this stability can be ameliorated with an improvement of the implant design. For example, the rounding of the rack teeth would permit the reduction of the stress concentration.

Regarding the shear mechanical test, the values for Device 1 were higher than for Device 2. This can be explained by the higher robustness of the device that restricts possible movement between its constituent parts. That is, in Device 2, there are small gaps between its parts allowing for the upper structure to slide when lateral loading is applied, not causing many stress concentrations points, unlike Device 1 where the parts have no room for movement.

Furthermore, the values for both mechanical tests results were found to be within the stipulated limit for the material that constitutes the device.

According to the Titanium Association, the material has an ultimate tensile strength of 910 MPa [15]. Thus, even though the mechanical tests are usually performed with a safety factor of 2, the material demonstrated to be able to mechanically withstand the applied loads.

4.2 Intact and Degenerative Models

The numerical prediction of RoM was done to evaluate the instability of the spine. With the IVD degeneration, this instability was verified.

As observed in Figure 4, in general, the predicted RoM values were significantly higher for the degenerative cases.

The undesired movement is often referenced in the literature as a consequence of the laxity of the AF fibers that will increasingly enhance the degeneration process [20,21].

However, the increase in RoM is not gradual with the severity of the degeneration process. Observing the RoM values for case 4, although higher than in the healthy case, they are not higher than in Cases 2 and 3. This is explained by the fact that, in moderate degeneration, the hardness of the disc is such that the laxity of the fibers turns out to be not so considerable and the movement ends up being restricted when compared to the others cases of degeneration.

The extension was where the RoM suffered the least impact. This phenomenon can be explained by the fact that, in this particular movement, there is a large intervention of facet joints, which restrict and limit the

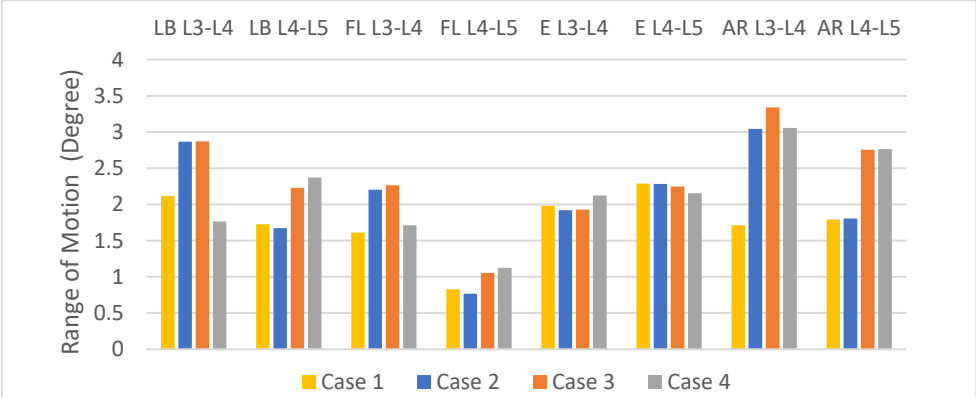

Figure 4: RoM Values of the Cases 1, 2, 3 and 4, at the different loading conditions: Lateral Bending (LB), Flexion (FL), Extension (E) and Axial Rotation (AR) for L3-L4 and L4-L5 segments.

movement, not allowing a large range of spinal extension. Also, the non-implementation of ligament degeneration may contribute to this result.

The separation of the RoM values for the two segments was made in order to understand the consequences for the adjacent levels at the time of IVD degeneration. Moreover, the mechanism of adjacent segment degeneration is not yet fully clarified [22]. Analyzing Figure 4 once more, in particularly the Cases 1 (healthy) and 2 (no degeneration in the level L4-L5), when the disc for segment L3-L4 is affected by a certain degree of degeneration there are consequences at the adjacent level L4-L5, a slight variation of RoM is observed and should be considered. The higher segmental difference was observed when degeneration occurs in this same segment, as expected.

Also, the values of the stresses (S33) in the NP and AF were studied to better understand the degeneration process. The comparison between all the degenerative cases are represented in Figures 5 (a) and (b).

According to the Figure 5(a), the stress observed in the center portion of the NP increased, in modulus, with the degeneration. This increment is associated with the stiffness of the nucleus matrix, that has been increased to simulate all degeneration stages. This variation is much more obvious in the segmental levels where the degeneration was applied. For example, observing the lateral bending movement in the L3-L4 level, it is possible to verify that the tension has increased in Case 2 relatively to the Healthy Case, but there was no increase in Case 3 over Case 2. This occurs as there is no degeneration progress in L3-L4 segment between Case 2 and Case 3, only verified the for LB L4-L5.

Another observation associated with some results already discussed for Figure 4, is the fact that in Case 3, the most severe case of degeneration, the stress values do not increase as much when compared with the other cases. This may be associated once again with the most noticeable influence of the increased IVD matrix stiffness relatively to the AF fibers laxity. Thus, the AF characteristics also have consequences at the NF level, confirming that the IVD adapts as a whole.

Comparing the extension with the other movements, the stress increase is not so considerable. This confirms what has already been observed in the analysis of the RoM, that the extension movement is very restricted by the posterior portion of the vertebra. Therefore, with the IVD degeneration, the instability of the spine does not constitute a large impact in this particular movement.

In Figure 5(a), one can also verify the adjacent segment influence. Although between Case 2 and Case 3 there is no change in the level of degeneration for the L3-L4 segment, there is a slight variation in the stress values obtained for the flexion movement. Thus, this proves that the degeneration of a given level has consequences in the adjacent levels, leading to mechanical stimulation and consequently to the propagation of this degeneration through the spinal column.

Analyzing the results for the Figure 5(b), it is possible

(a)

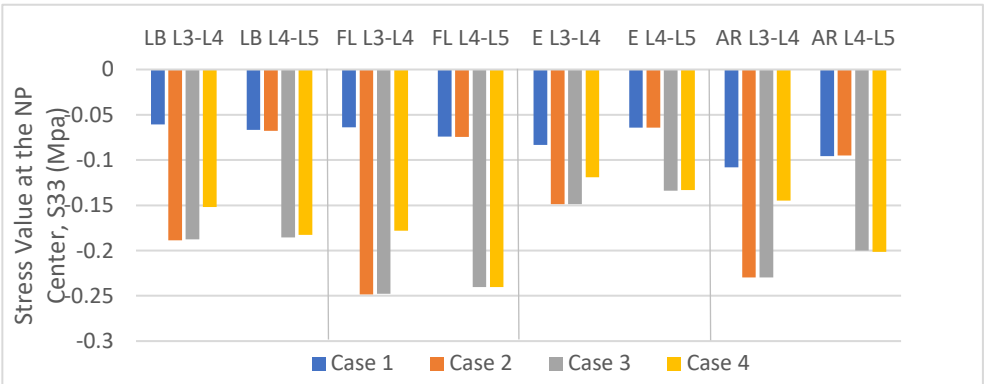

(b)

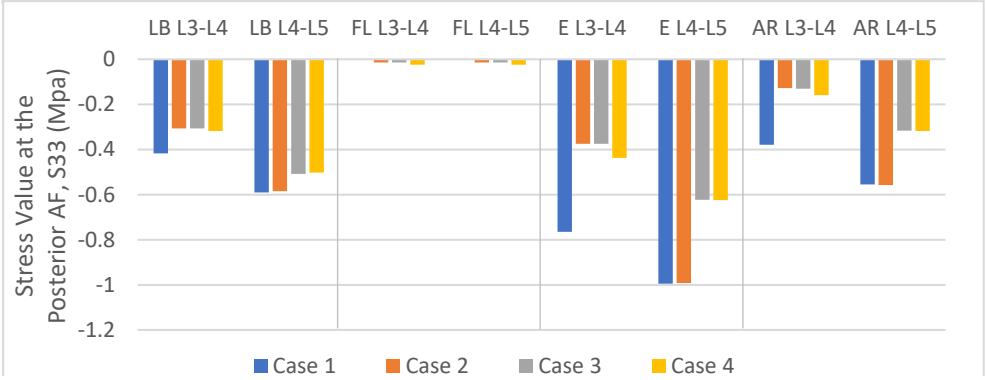

Figure 5: Stress Values of the Cases 1, 2, 3 and 4, at the different loading conditions: Lateral Bending (LB), Flexion (FL), Extension (E) and Axial Rotation (AR) for L3-L4 and L4-L5 segments: (a) at the NP center; (b) at the Posterior AF

to observe a general decrease of the stress in the AF. Despite the hardness of the AF matrix, it is possible to observe the high influence of the fibers' laxity due to the considerable decrease in stress along the AF. Many studies report that the reduction of intradiscal pressure reduces the tension in annulus fibers and increases the inward and outward bulging. Although the modelling of this model does not take pressures into account and, therefore, these cannot be measured, it is known that the results behaved as expected. In Figure 5 (b), the higher stress values are associated to the extension movement. But in this case, it is normal, since the stress is associated with a certain node of the posterior part of the AF, where there is a higher impact from the moment applied. On the other hand, stress values for flexion are the lowest.

Again, resuming the discussion above for the NP, it is also possible to observe in the graphic a slight decrease in stress for case 4, once again due to the higher influence of the increased stiffness in the AF comparatively to the weakening of the fibers. In addition, there is again a small influence on the stress values at the level adjacent to the degeneration.

Regarding the Cases 5 and 6, not represented, these RoM and Tension evaluations were also done and a high RoM was verified. This factor was studied to see the influence of considering the fibers laxity, and understand that there are several degeneration processes, and a lot of causes that can potentiate it.

4.3 Instrumented Models

For this section, only the Case 3 results are showed and discussed since the all cases proved to be quite similar to each other and followed the same trend.

RoM results, observed in Figure 6(a), the instrumented segment L3-L4 verified a very large restriction of movement. The RoM decreased considerably, compared to the unhealthy model, as well as compared to the healthy model. This restriction is expected since the purpose of these devices is a segmental fixation.

Here, there is a degeneration at the segment L4-L5, and this is evidenced by the increase of RoM, being more evident in lateral bending indicating that, for the L4-L5 level, movement reduction is not achieved.

(a)

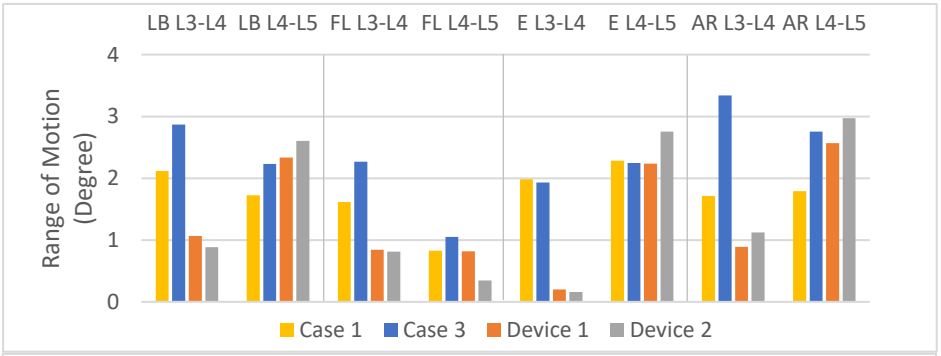

(b)

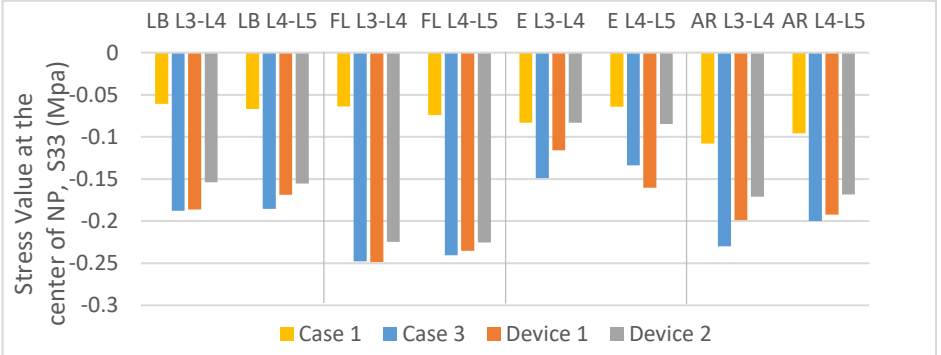

(c)

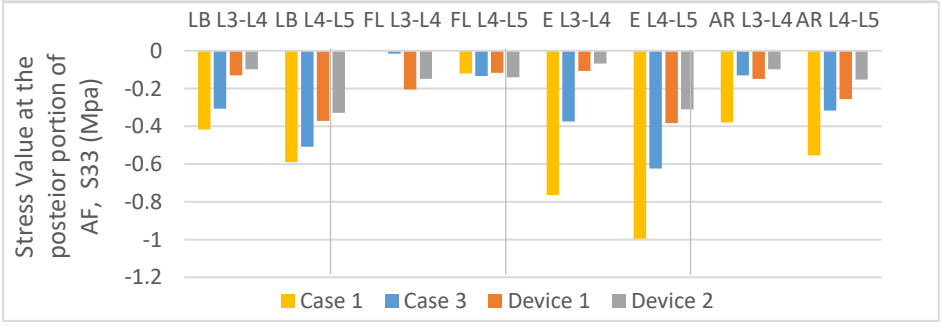

Figure 6: RoM and Stress Values of the Cases 1, 3, and Case with Device 1 and Device 2 implemented, at the different loading conditions: Lateral Bending (LB), Flexion (FL), Extension (E) and Axial Rotation (AR) for L3-L4 and L4-L5 segments: (a) RoM values; (b) Stress at the NP center; (c) Stress at the Posterior AF.

This is due to the fact that the instrumentation is implemented at the L3-L4 level and it mostly restricts this segment. In extension, the opposite is also verified as well as for flexion with Device 1, but more lightly in this case. This may be associated with the fact that interspinous fixators play a major role in restricting frontal movements, and that the high decrease in RoM at the instrumented level has a major influence on the adjacent segment. Moreover, with Device 2 there is even an increase in RoM over the unhealthy case, which is not intended and could lead to further instability and degeneration. RoM increase can be due to the need to establish spinal movement and guarantee the normal functionality of the spine.

Comparing the two devices, one can see that, in general, they behave quite similarly. They satisfy their purpose of restricting and correcting the column instability. Thus, since Device 1 is already used in actual surgical applications and meets all the necessary biomechanical prerequisites, this similar behavior observed in Device 2 turns out to be beneficial.

Observing now the stress results (S33) in the Figure 6(b), here the stress value decreased. contradicting the stress increase in the degenerative case. This reduction indicates a load relief of this IVD portion. The stress values for the devices do not reach the values of the healthy model, however it is considered that this stress reduction, and tendency for the healthy case results are favorable biomechanical factors. The degeneration retardation and the attempt to prevent disc replacement by a cage are the major goals when introducing the spinal fixators in the spinal column. Thus, these results support a good clinical performance. These ambitious results are more evident in the model with Device 2, proving to be a great asset in their biomechanical performance. The degeneration in the L4-L5 segment demonstrates stress variation between Case 3 and the two devices. In addition, although this segment is not instrumented, it also undergoes significant improvements, as the stress also decreases to values closer to the healthy model. This is most noticeable on Device 2 for all movements. So, once more, it is possible to affirm the good performance of the device.

In Figure 6(c), the same results are illustrated but for the posterior portion of the AF. Here, the contradiction of the degeneration state is no longer so evident. which can be explained by the large load supported by the device in these movements. The AF fibers, with laxity, are not able to withstand the load and this is being directed towards the device. However, despite of the wide range of results, Device 1 and Device 2 behave very similarly in all cases. Since Device 1 is already clinically approved, then the similar mechanical behavior of Device 2 relatively to Device 1, is an aspect in favor for the new concept device.

4.5 Discussion Summary

In this study, several parameters were studied to achieve the proposed goal.

Considering at first the Axle® and innovative devices in separate, both showed a safety performance in the mechanical tests usually used for this purpose. Their stress values were below the maximum stipulated for the material constituting this type of medical device. However, some results observations must be taken into considerations when proposing a final design for the new innovative device, since this one, evaluated in this study, was just a concept for a new interspinous fixators inspired by Axle®. This means that some effects are fairly important, such as the stress concentration in the rack teeth, to the success of the surgery.

In relation to the analysis of the spinal degeneration the balance and relation between the fibers laxity and matrix stiffness that were used to simulate the degeneration development, were evidence, where there was verified the influence of disc dehydration, in relation to the loss of elasticity of the AF fibers. Thus, it is important to mention that, to the authors knowledge, this is the only FE study in the literature that had in consideration the fibers laxity while increasing the stiffness of the IVD to simulate the degenerative process, although it was already mentioned and suggested in some studies This observation can be highly important in the study of the different cases of spinal degeneration.

Regarding the instrumented models, it was observed a similar trend for both devices. The high movement restriction which enables higher stability of the instrumented segment, the reduction of the NP stress to values nearly to the healthy ones, and the reduction in AF stress that accomplish the obtained values for Device 1, all prove the good biomechanical performance of the innovative device, indicating what could be a viable option to be used instead of the Axle® device.

5. Conclusions and Limitations

It was considered that the new device showed that it can be potentially used over the original implant, and further tests and studies should be done to better prove its clinical use, demonstrated to be a good investment focus by companies focused on the design, development and commercialization of spinal fixation systems. This is an important conclusion, since this device design can reduce significantly the risk associated to the surgical procedure and can be worth to be adopted in cases in which the specialist has higher difficulty in inserting the device correctly, enabling him to do it only once.

This work and the models that were constructed presents some limitations that can be discussed and can be addressed to possible future works. A better IVD modelling could be considered, as well as, the consideration of others mechanical changes such as the ligaments properties modifications in the spinal degeneration simulation.

6. Acknowledges

To all those who made it possible: Supervisors, friends and family.

7. References

[1] L. Zhu and J. Yin, “Interspinous fusion device : A systematic review of clinical and biomechanical evidence,” vol. 8, no. 11, pp. 1–12, 2016

[2] P. Gédet, D. Haschtmann, P. A. Thistlethwaite, and Æ. S. J. Ferguson, “Comparative biomechanical investigation of a modular dynamic lumbar stabilization system and the Dynesys system,” *Eur. Spine J.*, pp. 1504–1511, 2009.

[3] T. Oktenoglu *et al.*, “Pedicle screw-based posterior dynamic stabilisation of the lumbar spine: in vitro cadaver investigation and a finite element study,” *Comput. Methods Biomech. Biomed. Engin.*, vol. 18, no. 11, pp. 1252–1261, 2015.

[4] S. A. Gonzalez-Blohm, J. J. Doulgeris, K. Aghayev, W. E. Lee, A. Volkov, and F. D. Vrionis, “Biomechanical analysis of an interspinous fusion device as a stand-alone and as supplemental fixation to posterior expandable interbody cages in the lumbar spine,” *J. Neurosurg. Spine*, vol. 20, no. 2, pp. 209–219, 2013.

[5] R. Korez, B. Ibragimov, B. Likar, F. Pernus, and T. Vrtovec, “A Framework for Automated Spine and Vertebrae Interpolation-Based Detection and Model-Based Segmentation,” *IEEE Trans. Med. Imaging*, vol. 34, no. 8, pp. 1649–1662, 2015.

[6] S. Naserkhaki, N. Arjmand, A. Shirazi-Adl, F. Farahmand, and M. El-Rich, “Effects of eight different ligament property datasets on biomechanics of a lumbar L4-L5 finite element model,” *J. Biomech.*, vol. 70, pp. 33–42, 2018.

[7] B. Weisse, A. K. Aiyangar, C. Affolter, R. Gander, G. P. Terrasi, and H. Ploeg, “Determination of the translational and rotational stiffnesses of an L4-L5 functional spinal unit using a specimen-specific finite element model,” *J. Mech. Behav. Biomed. Mater.*, vol. 13, pp. 45–61, 2012.

[8]F. Heuer, H. Schmidt, Z. Klezl, L. Claes, and H. J. Wilke, “Stepwise reduction of functional spinal structures increase range of motion and change lordosis angle,” *J. Biomech.*, vol. 40, no. 2, pp. 271–280, 2007.

[9] R. J. G. D. Guerreiro, “Biomechanical effects of different lumbar fusion cage designs,” 2018.

[10] A. Castro, “Development of a biomimetic finite element model of the intervertebral disc diseases and regeneration,” 2013.

[11] A. M. Ellingson, M. N. Shaw, H. Giambini, and K. N. An, “Comparative role of disc degeneration and ligament failure on functional mechanics of the lumbar spine,” *Comput. Methods Biomech. Biomed. Engin.*, vol. 19, no. 9, pp. 1009–1018, 2015.

[12] B. Yu, C. Zhang, C. Qin, and H. Yuan, “FE modeling and analysis of L4-L5 lumbar segment under physiological loadings,” *Technol. Heal. Care*, vol. 23, pp. S383–S396, 2015.

[13] R. Eberlein, G. A. Holzapfel, and M. Fröhlich, “Multi-segment FEA of the human lumbar spine including the heterogeneity of the annulus fibrosus,” *Comput. Mech.*, vol. 34, no. 2, pp. 147–163, 2004.

[14] X. S. Innovations, “X-spine Surgical Technique,” 2012.

[15] F. E. Dition *et al.*, *International Titanium Association- Specifications Guide*, Fourth Edi. 2005.

[16] Z. C. Zhong, S. H. Wei, J. P. Wang, C. K. Feng, C. S. Chen, and C. H. Yu, “Finite element analysis of the lumbar spine with a new cage using a topology optimization method,” *BMC Musculoskelet. Disord.*, vol. 28, no. 1 SPEC. ISS., pp. 90–98, 2008.

[17] F. Galbusera, H. Schmidt, and H. J. Wilke, “Lumbar interbody fusion: A parametric investigation of a novel cage design with and without posterior instrumentation,” *Eur. Spine J.*, vol. 21, no. 3, pp. 455–462, 2012.

[18] S. Naserkhaki, J. L. Jaremko, and M. El-rich, “Effects of inter-individual lumbar spine geometry variation on load-sharing : Geometrically personalized Finite Element study,” *J. Biomech.*, vol. 49, no. 13, pp. 2909–2917, 2016.

[19] S. Naserkhaki, J. L. Jaremko, S. Adeeb, and M. El-Rich, “On the load-sharing along the ligamentous lumbosacral spine in flexed and extended postures: Finite element study,” *J. Biomech.*, vol. 49, no. 6, pp. 974–982, 2016.

[20] C. Cavalcanti, H. Correia, A. Castro, and J. L. Alves, “Constituive modelling of the annulus fibrosus: Numerical implementation and numerical analysis,” vol. 7, pp. 3–6, 2013.

[21] L. M. Ruberte, R. N. Natarajan, and B. G. Andersson, “Influence of single-level lumbar degenerative disc disease on the behavior of the adjacent segments — A finite element model study,” *J. Biomech.*, vol. 42, pp. 341–348, 2009.

[22] S. Jiang and W. Li, “Biomechanical study of proximal adjacent segment degeneration after posterior lumbar interbody fusion and fixation: A finite element analysis,” *J. Orthop. Surg. Res.*, vol. 14, no. 1, pp. 1–7, 2019